Impact of Imaging Geometry on 3D Geopositioning Accuracy of Stereo Ikonos Imagery

Rongxing Li, Xutong Niu, Chun Liu, Bo Wu, and Sagar Deshpande

Abstract

Special Ikonos data acquisition and investigation were conducted to study the relationship between three-dimensional (3D) geopositioning accuracy and stereo imaging geometry, in particular, convergence angles. Six Ikonos images (four on one track and two on another track) were collected for a test site at Tampa Bay, Florida, in 2004 and 2007, respectively. Different combinations of Ikonos stereo image pairs, both along-track and cross-track, were formed. Using the high-resolution satellite image processing system developed at The Ohio State University, DGPS (Differential Global Positioning System) controlled ground control points, and a number of check points, we demonstrated: (a) The convergence angle plays an important role in along-track or cross-track stereo mapping, especially in improvement of the accuracy in the vertical direction; (b) Regardless of stereo configuration (along-track or cross-track), the accuracy in the X (cross-track) direction is better than that in the Y (along-track) direction; and (c) Although there is a slight correlation between the convergence angle and the accuracy in the Y (along-track) direction in the case of along-track stereo configuration, no distinct relationship is found in the X (cross-track) direction. Similarly, improvement of the horizontal accuracies is found with increased convergence angles when dealing with cross-track stereo pairs.

Introduction

In September 1999, GeoEye's Ikonos Earth-imaging satellite was successfully launched. Carrying the first commercially available high-resolution satellite imaging system, it initiated a new era of civilian Earth observation and digital mapping using high-resolution satellite imagery (Li, 1998). High-resolution satellite imagery (HRSI) such as that provided by Ikonos (1-meter resolution) and QuickBird (sub-meter resolution) has been widely used in the past several years for digital topographic mapping and surveying (Li *et al.*, 2003 and 2007; Noguchi *et al.*, 2004). Imaging geometry has played an important role in deriving accurate geopositioning information from such HRSI imagery (Di *et al.*, 2003a; Fraser and Hanley, 2003; Wang *et al.*, 2005; Li *et al.*, 2007). A thorough investigation and understanding of the relationship between imaging geometry and geopositioning accuracy can provide both a practical and theoretical basis when planning image acquisition or selecting image pairs for accurate 3D mapping from stereo satellite imagery.

Several sensor models, including rigorous and rational function sensor models, have been presented to describe the geometrical relationships between imaged objects and the corresponding HRSI scene (Fraser, 1999; Tao and Hu, 2001; Di *et al.*, 2003a; Tao *et al.*, 2004; Wang *et al.*, 2005; Habib *et al.*, 2007). The rigorous sensor model explicitly uses both the internal and external characteristics of the imaging sensor to faithfully represent the geometry of the scene formation. However, in many cases it may not be a computationally efficient model because of its sophisticated parameter definition, complex expression, and self-correlation of model parameters (Li *et al.*, 2007; Habib *et al.*, 2007). On the other hand, for several reasons a rigorous sensor model may not be provided by the image supplier and instead, a rational function model (RFM) may be provided. The additional merits of the RFM are that it can be used as an alternative to the rigorous sensor model and has its independence of sensor parameters when being used. Ground coordinates derived from the RPCs, such as those from the Ikonos product, showed a ground error of about 16 m to 25 m, mainly as a systematic shift (Di *et al.*, 2003b; Li *et al.*, 2003 and 2007). A similar result was reported by Fraser and Hanley (2003).

The nature of the above geopositioning error allows the development of methods that can be used to generate high accuracy mapping products at a low cost from such basic imagery products as Ikonos' Geo or QuickBird's Basic Imagery. The ground accuracy of these products can be enhanced through the use of simply a few good quality ground control points (GCPs) (Zhou and Li, 2000; Niu *et al.*, 2004; Wang *et al.*, 2005; Aguilar *et al.*, 2007). For example, Dial (2000) estimated the stereo mapping accuracy of Ikonos products with GCPs of 1.32 m RMSE in the horizontal direction and 1.82 m RMSE in the vertical direction. Di *et al.* (2003b) used a 3D affine transformation model to refine the

Rongxing Li, Bo Wu, and Sagar Deshpande are with the Mapping and GIS Laboratory, Department of Civil and Environmental Engineering and Geodetic Science, The Ohio State University, Columbus, OH 43210-1275 (li.282@osu.edu).

Xutong Niu is with the Department of Math, Physics, Computer Science, and Geomatics, Troy University, Troy, AL 36082.

Chun Liu is with the Department of Survey and Geo-Informatics, Tongji University, Shanghai, China, 200092.

Photogrammetric Engineering & Remote Sensing
Vol. 75, No. 9, September 2009, pp. 1119–1125.

0099-1112/09/7509–1119/$3.00/0

RPC-derived ground coordinates for Ikonos images and achieved an accuracy of 1.5 m in planimetry and 1.6 m in height. Wang *et al.* (2005) compared the results of different methods in both image space and object space, including different transformation models with different GCP distributions, to improve Ikonos stereo geopositioning accuracy. The results showed that the affine transformation can produce better accuracies when used with four to six evenly distributed GCPs. Furthermore, Li *et al.* (2007) investigated the attainable ground accuracy through integrating Ikonos and QuickBird images to form image pairs with different pointing geometries. It was found that the integration of Ikonos and QuickBird images is feasible and can improve the 3D geopositioning accuracy using a proper combination of stereo images. It was also found that satellite imaging geometry plays a significant role in improving ground accuracy. They also noticed that the ground accuracy is related to some degree to the convergence angle of the image pairs. However, due to the limited number of stereo images in that study, an extensive investigation on the impact of the convergence angle on geopositioning accuracy was not possible.

To explore the full potential of HRSI, an in-depth investigation of the relationship between imaging geometry and geopositioning accuracy, particularly the convergence angle issue, is essential for optimal image acquisition planning. For instance, in the planning stage of image acquisition, there is always a major concern as to which combination of a stereo pairs of images can produce the highest geopositioning accuracy. To fully address this important issue and to further the work of Li *et al.* (2007), this paper investigated the attainable 3D geopositioning accuracy of various image pairs with different stereo geometries by using Ikonos images specially collected for this purpose from two tracks above Tampa Bay, Florida. A variety of combinations of Ikonos stereo configurations, including along-track and cross-track stereo, are studied and analyzed.

Imaging Geometry and Data Acquisition

Supported by GeoEye, an experiment was designed and carried out to collect the desired Ikonos images at Tampa Bay, Florida in November 2007 with various pointing angles of five images (four succeed in the end) along one orbital track. The data set also includes two existing Ikonos images of the same area acquired in July 2004.

The along-track Ikonos stereo images were designed to create along-track stereo pairs with various convergence angles (Figure 1a). The imaging area is given by a defined rectangle; the azimuth angle and elevation angle of the area with respect to each satellite position of the five images need to be determined with consideration of orbital geometry. In this study, the convergence angles between two adjacent images are designed to be 15° so that the maximum convergence angle between the first image (satellite position A) and the last one (satellite position E) is 60°. The third image in the sequence (satellite position C) has the highest elevation angle. In the image acquisition process, the elevation angle and azimuth angle are two very important parameters for adjusting the sensor pointing. In order to achieve the desired convergence angle of 15° between adjacent images, it is necessary to establish the relationship between the convergence angle and the corresponding elevation and azimuth angles for each image in the imaging area.

Before image acquisition, the satellite orbit track and its ground track in the area can be determined based on collection date and satellite ephemeredes (Figure 1a and 1b). As shown in Figure 1b, Point O is the center of Earth, Point P is the image center, and Point C is the orbit position of the third image; correspondingly, C′ is the nadir point of Point C on the ground track. Hence, PC′ is perpendicular to the ground track. The orbit height of the satellite is known (681 km) as is the azimuth angle of the ground track (8.3°). Thus, the azimuth of Position C with respect to image center P is 98.3° since P is on the west side of the ground track (otherwise it would be 278.3°, as P is on the east side of the ground track). The distance between the image center P and nadir Point C′ can be estimated by the user and refined by GeoEye Company. Using the known orbit height, the elevation angle can be calculated. The actual elevation of orbit position C is 85.781° calculated from the metadata of the image. The next orbit Position D can be derived based on the predefined convergence angle ($\delta = \angle CPD = 15°$) between the two images using the following equation:

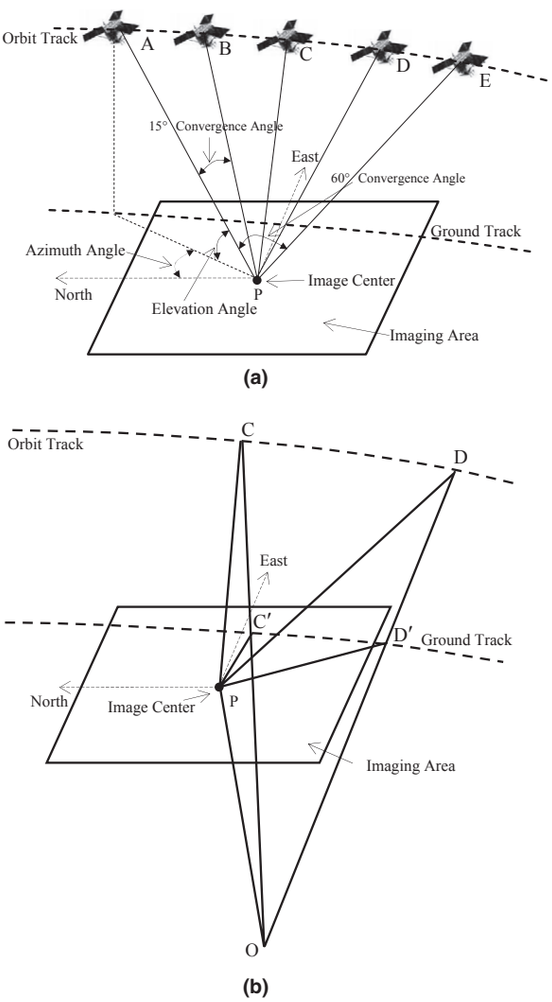

Figure 1. Imaging geometry of the stereo Ikonos images: (a) Imaging area, convergence angle, and pointing parameters, and (b) imaging geometry of a two-image stereo pair.

$$\alpha = 98.3^\circ + \arccos\left(\frac{1 + \cos(Dist_{PC'}/R) - A - B}{2\sqrt{(1-A)(1-B)}}\right) \qquad (1)$$

$$\theta = \arccos((1 + H/R)\sin\beta)$$

where, α is the azimuth from Position P to Position D, θ is the elevation of the Position D, H is the orbit height of the satellite, R is the radius of the Earth, and

$$\beta = \arccos(((R+H)^2 + s^2 - R^2)/(2s(R+H)))$$

$$s = \sqrt{R^2 + (R+H)^2 - 2R(R+H)\cos(Dist_{PC'}/R)}/\cos\delta$$

$$A = (a + b + \sqrt{b^2 - 4ac})/a$$

$$B = (2R^2 + 2(H+R)^2 + s\sin\beta - 2R(H+R)A)/(2R(H+R)).$$

$$C = \arcsin(R\sin(Dist_{PC'}/R)/s)$$

$$a = 4(H+R)\cos^2 C/\cos^2\delta$$

$$b = -4s(H+R)\tan^2\delta\cos C - 4(H+R)^2$$

$$c = s2(1+\tan^2\delta)\sin^2\delta$$

Consequently, the five satellite positions were calculated with the expected convergence angles of 15° between adjacent images, 30° between every other image, 45° between every second image, and 60° between the first and the last images.

The designed experiment was carried out on 09 November 2007. Four panchromatic Ikonos images with a resolution of about 0.85 m were taken by GeoEye. Because of weather conditions and scheduling and tasking issues, the planned fifth image was not taken. Therefore, we incorporated the two existing Ikonos images collected at July 2004 into the data set of the four newly acquired Ikonos images to form both along-track and cross-track stereo image configurations. Table 1 summarizes the data acquisition information of the newly acquired and the existing images.

Figure 2 illustrates the actual satellite positions at the times when the images were taken. The two tracks and six orbit positions of the new images (1 to 4) and existing images (5 to 6) are illustrated in an azimuth-elevation diagram in Figure 2. The two sets of images are acquired from two different tracks that are approximately 200 km apart. The actual convergence angle (Li *et al.*, 2007) between every two images that have azimuth and elevation values as (α_1,θ_1) and (α_2,θ_2) can be calculated as:

$$\cos\delta = \sin\alpha_1\sin\alpha_2 + \cos\alpha_1\cos\alpha_2\cos(\theta_2 - \theta_1). \quad (2)$$

In Table 2, we list convergence angles of stereo pairs with all combinations of new images along-track. Similarly, the convergence angles with all combinations between the new and existing images are also listed as cross-track convergence angles, all in ascending order.

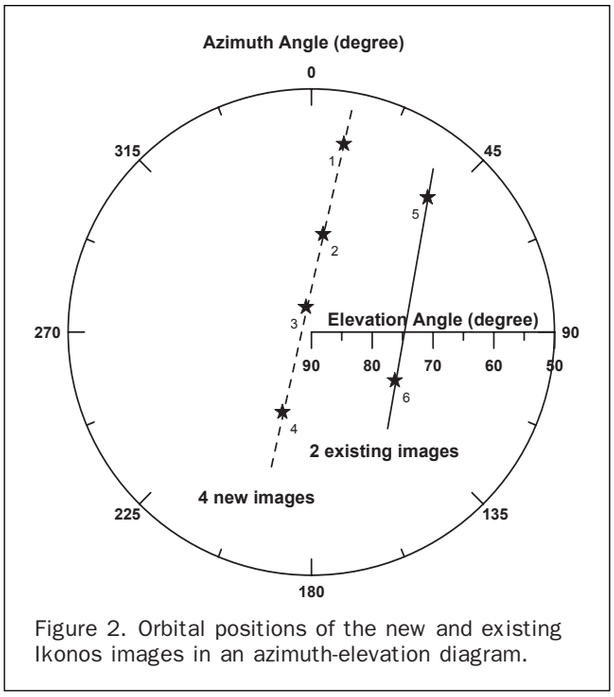

Figure 2. Orbital positions of the new and existing Ikonos images in an azimuth-elevation diagram.

Table 2. Along- and Cross-track Convergence Angles

Along-track		Cross-track	
Image Combination	Convergence Angle	Image Combination	Convergence Angle
2 and 3	12.311°	1 and 5	15.635°
1 and 2	15.210°	2 and 5	18.018°
3 and 4	17.691°	3 and 6	18.954°
1 and 3	27.521°	4 and 6	19.072°
2 and 4	30.002°	2 and 6	26.690°
1 and 4	45.212°	3 and 5	26.906°
		1 and 6	39.484°
		4 and 5	42.576°

Analysis of Geopositioning Accuracy

A systematic experiment was designed to investigate the relationship between the convergence angles and the geopositioning accuracy of different Ikonos image pairs. In general, Ikonos stereo images have a stable imaging geometry and a geopositioning accuracy of around one meter has been reported after a translation of linear correction in either the image or object space (Di *et al.*, 2003b; Fraser and Hanley, 2003). In this study, a simple translation model in the image space was used to correct the systematic errors and to improve the geopositioning accuracy of Ikonos imagery:

$$I' = I + a$$
$$J' = J + b \quad (3)$$

Table 1. Data Acquisition Information of the Ikonos Images used in the Experiment

Image set	Image ID	Acquisition Date and Time (GMT)	Image Size (row * column)	Collection Azimuth (θ)	Collection Elevation (α)
New images	1	09-11-2007 16:20	10052*14528	9.817°	58.611°
	2	09-11-2007 16:21	10052*14528	6.813°	73.778°
	3	09-11-2007 16:21	10052*14528	347.720°	85.781°
	4	09-11-2007 16:21	10052*14528	199.927°	76.019°
Existing images	5	08-07-2004 16:17	8484 * 12160	40.799°	60.753°
	6	08-07-2004 16:18	8484 * 12160	120.105°	74.141°

where I' and J' are the corrected image coordinates and I and J are the image coordinates derived by using the RPCs provided in the image metadata; a and b are translational corrections that can be determined by the ground control points (GCPs). Two GCPs are measured by DGPS surveying to correct the translations a and b, and to improve the quality of the final result. Consequently, checkpoints (CKPs) determined by GPS or bundle adjusted aerial triangulations were employed to compute RMSEs and to evaluate the geopositioning accuracies of different Ikonos image stereo combinations. Figure 3 summarizes the data processing procedure used to perform this study. As shown in Figure 3, only six combinations of cross-track stereo pairs with various convergence angles were selected from the eight possible combinations listed in Table 2. This is because that the other two combinations (Images 4 and 6, and Images 2 and 6 in Table 2) have their convergence angles very close to the others and therefore, are excluded.

Geopositioning Accuracy of the Along-track Image Pairs

Figure 4 is one of the four new Ikonos images acquired in November 2007. As shown in Table 2, six along-track stereo pairs can be formed from the four images. Two GPS points (triangles in Figure 4) were used as GCPs to process each image and correct translational errors. There are six additional GPS points (squares) and seven points (circles) determined by bundle adjustment of aerial photographs covering the entire area, which were employed as CKPs.

Furthermore, the GPS points were measured by using the Real Time Kinematic (RTK) mode of the DGPS (Differential Global Positioning System) technique. Two mobile GPS receiver units were used to survey the points and receive the real-time corrections provided by a reference station in the area, for which we have known coordinates as a reference to the global coordinate system. The mobile GPS units receive phase information of the carrier signals broadcasted from the reference station and compare them with that received at the local points. This allows the mobile GPS units to calculate their positions at a higher accuracy with respect to the reference station (Monteiro *et al.*, 2005). The average errors of these determined GPS points are 0.014 m in the X direction (easting), 0.017 m in the Y direction (northing), and 0.028 m in the Z (vertical) direction. The non-GPS CKPs are mainly distinctive image features such as road intersections, building corners, and other objects. Their image coordinates are identified at a sub-pixel level. A photogrammetric aerial image bundle adjustment with 24 images was performed successfully, where the CKP coordinates are a part of the unknowns and are solved for (Li *et al.*, 2007). After the bundle adjustment, we achieved a ground accuracy of the CKPs of 0.153 m in the X direction, 0.195 m in the Y direction, and 0.067 m in the Z direction, which are appropriate for checking the ground positioning accuracy for this study.

The coordinates of the two GCPs in both the image and object spaces were used to calculate the translation coefficients in Equation 2 for each image (Figure 3). These were subsequently used to refine the image coordinates of the CKPs. The ground coordinates of these CKPs were then calculated from their refined image coordinates and RPCs of the images involved forming individual stereo pairs. Finally, the RMSE was computed from these CKPs for each stereo pair by comparing the computed ground coordinates to the known ground coordinates in X, Y, and Z directions (Table 3).

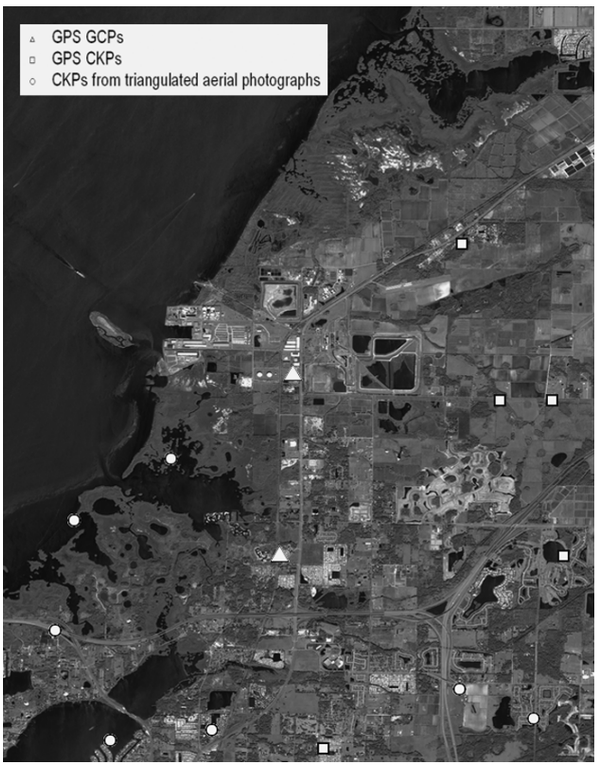

Figure 4. One of the four new Ikonos images with GCPs (triangles) and CKPs (squares and circles).

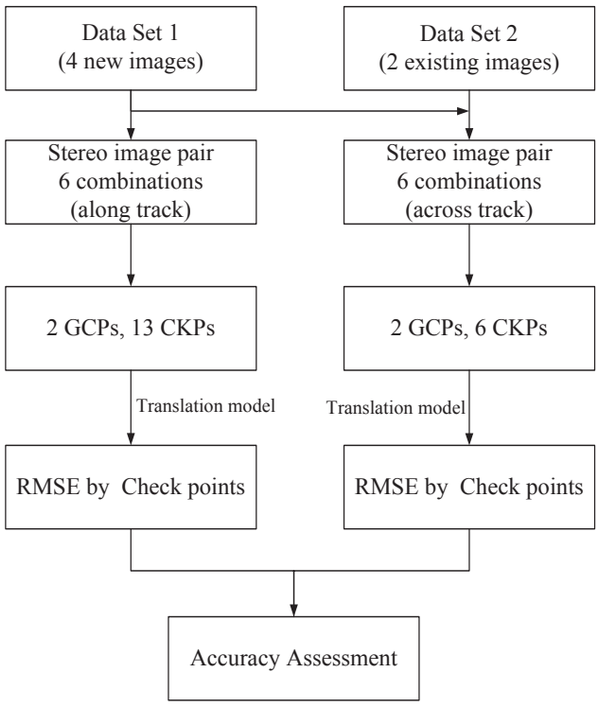

Figure 3. Data processing flow chart for geopositioning accuracy analysis.

TABLE 3. GEOPOSITIONING ACCURACY OF THE ALONG-TRACK STEREO IMAGE PAIRS VERSUS CONVERGENCE ANGLES

Along-track Stereo Combination			3D Geopositioning Accuracy (RMSE: meters)		
ID	Images	Convergence Angle (δ_i)	σ_x	σ_y	σ_z
1	2 and 3	12.311°	0.511	1.506	2.949
2	1 and 2	15.210°	0.568	1.454	2.362
3	3 and 4	17.691°	0.768	1.151	2.321
4	1 and 3	27.521°	0.445	1.392	1.895
5	2 and 4	30.002°	0.554	0.980	1.502
6	1 and 4	45.212°	0.525	1.055	0.691

From Table 3 and Figure 5, it can be clearly seen that, for the along-track Ikonos image pairs, there is a strong correlation between the convergence angle and the vertical accuracy, with a significant improvement of the vertical accuracy from 2.9 m at a convergence angle of 12.3° to 0.7 m at 45°. For the same convergence angle increasing, there is only a slight improvement of accuracy in the *Y* direction (along-track), from 1.5 m to 1.1 m. That indicates that the increase of the along-track convergence angle has some improvement in imaging geometry for along-track coordinate determination. Finally, no distinct correlation was observed between the accuracy of the *X* coordinates (cross-track) and the convergence angle. That suggests that the increase of the convergence angle in the along-track direction has little impact on the triangulation capability in the *X* direction.

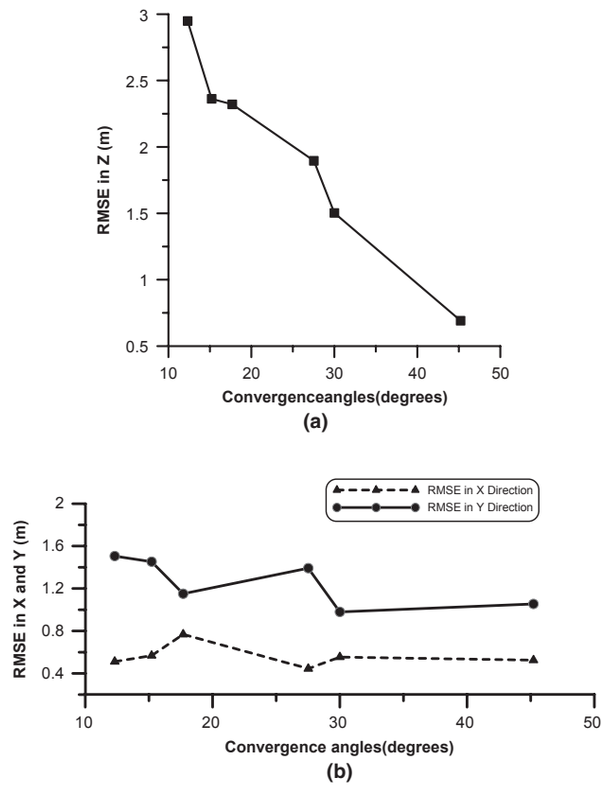

Figure 5. Geopositioning accuracy of the along-track stereo image pairs versus convergence angles: (a) vertical correlation, and (b) horizontal correlation.

Geopositioning Accuracy of the Cross-track Image Pairs

The cross-track stereo pairs are formed by the four new images on one track and the two existing images on another track acquired in July 2004, one of which is shown in Figure 6. Six combinations of cross-track stereo pairs with various convergence angles were selected from the eight possible combinations listed in Table 2. The same two GPS points (triangles in Figure 6) used in the along-track analysis

Figure 6. One of the two existing Ikonos images with GCPs (triangles) and CKPs (circles).

were used again as GCPs. However, there were clouds in the boundary area of the two existing images; also those images were acquired three years earlier on a different track. In many cases, it was either impossible or difficult to identify common features in the overlap area of the cross-track stereo pairs. We were unable to use the same 13 CKPs employed in the along-track stereo pair experiments. Instead, we selected six new CKPs (circles in Figure 6) that can be identified in all the cross-track images, and are distributed reasonably evenly in the test area. Their ground positions were determined by using bundle adjusted aerial photographs.

In the cross-track case, a convergence angle is formed by one optical ray from one track and the other from a different track. The pointing information came separately with the two datasets. Using the same methods performed in the experiment with along-track stereo pairs, the 3D geopositioning accuracies in the *X*, *Y*, and *Z* directions of the cross-track stereo pairs were computed for each stereo pair using the GCPs and CKPs. The results are listed in Table 4 and illustrated in Figure 7.

Again, there is a clear correlation between the convergence angle and the vertical accuracy shown in Table 4 and Figure 7a where the accuracy is improved from 1.9 m at a convergence angle of 15.6° to 1.0 m at 42.6°, although this improvement is not as significant as that in the experiment with the along-track stereo pairs.

By observing Tables 3 and 4 and Figures 5 and 7, it can be seen that the accuracy in the *X* direction (cross-track) is generally higher than that in the *Y* direction (along-track) in both cases. This is also consistent with the analysis and results published previously (Lutes and Grodecki, 2004; Li *et al.*, 2007). The phenomenon may be caused by the fact that polynomials (up to third order) are used to model the three attitude angles of the camera system (Li, 1998); the cross-track angle (roll) may not change much from the orbital dynamics point of view and can be modeled by the polynomial; on the other hand, the along-track angle (pitch) changes as the satellite moves on the orbit and may be more affected spacecraft vibration, which cannot be completely compensated by the polynomial. Further study is needed on the in-depth reasons and how this directly affects the along-track geopositioning accuracy.

It should be noted that in Table 3 and Figure 5b for the along-track case, the accuracy in the *Y* direction (along-track) improves as the along-track convergence angle increases. Furthermore, as illustrated in Figure 7b and Table 4 for the cross-track case, there is also a general improvement of accuracy in the *Y* direction (along-track) as the convergence angle increases, although it is not very significant. The main reason for the latter case is that the convergence angles formed by the cross-track image pairs are also mainly in the along-track direction, except the combinations of image pairs 1 and 5, 2 and 5, and 3 and 6 (Figure 2; Table 4).

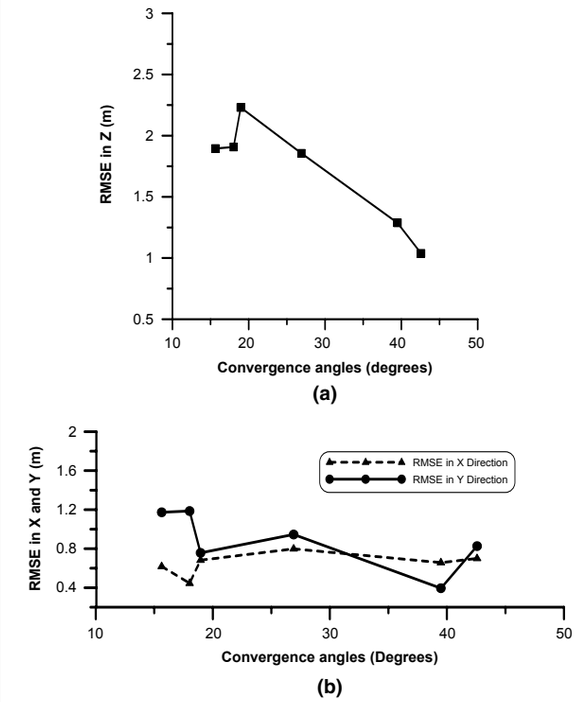

Figure 7. Geopositioning accuracy of the cross-track stereo image pairs versus convergence angles: (a) vertical correlation, and (b) horizontal correlation.

The above shows that, to some degree, the impact of the convergence angle on the horizontal accuracy also depends on the azimuth direction formed by the two optical rays. However, a substantial improvement of the horizontal accuracy is shown in average accuracy ratio (σ_y/σ_x) from about 2.3 (along-track case, Table 3) to about 1.4 (cross-track case, Table 4), i.e., more homogeneous horizontal accuracy.

Discussion and Conclusions

A specially designed experiment for testing the relationship between the 3D geopositioning accuracy and convergence angles was carried out. Six Ikonos images pointing at the same test region at Tampa Bay, Florida, were employed, four images on one orbital track acquired in November 2007, and the other two images on a different orbit track acquired in July 2004. Different combinations of stereo images were selected from among these six images, to build along-track and cross-track

TABLE 4. GEOPOSITIONING ACCURACY OF THE CROSS-TRACK STEREO IMAGE PAIRS VERSUS CONVERGENCE ANGLES

Cross-track Stereo Combination			3D Geopositioning Accuracy (RMSE: meters)		
ID	Images	Convergence Angle (δ_i)	σ_x	σ_y	σ_z
1	1 and 5	15.635°	0.618	1.173	1.895
2	2 and 5	18.018°	0.446	1.186	1.908
3	3 and 6	18.954°	0.682	0.757	2.231
4	3 and 5	26.906°	0.799	0.946	1.855
5	1 and 6	39.484°	0.657	0.395	1.288
6	4 and 5	42.576°	0.699	0.827	1.038

stereo pairs. GCPs determined by the DGPS techniques were employed to process the images. Assessments of 3D geopositioning accuracies were performed by using CKPs with along-track and cross-track stereo configurations. Based on the above discussion and results, the following can be concluded:

- Whenever possible, high-resolution satellite images, such as Ikonos images, for generation of 3D mapping products, should be selected or acquired with consideration of stereo imaging geometry, including convergence angles and along-track or cross-track stereo configuration, to improve the attainable ground position accuracy.
- For the along-track and cross-track Ikonos stereo pairs, it is clearly demonstrated that large convergence angles produced higher accuracies in the vertical direction. This is particularly significant in the along-track configuration.
- Regardless of stereo configuration (along-track or cross-track), the accuracy in the *X* (cross-track) direction is better than that in the *Y* (along-track) direction. This is also consistent with our previously published result using less comprehensive data (Li *et al.*, 2007).
- Although there is some correlation between the convergence angle and the accuracy in the *Y* (along-track) direction, no distinct relationship is found in the *X* (cross-track) direction. However, improvement of the horizontal accuracies is found with cross-track stereo pairs by providing more homogeneous accuracies in both along-track and cross-track directions.

Acknowledgments

The special data acquisition experiment was supported and carried out by GeoEye. We appreciate the collaboration by Mr. Gene Dial of GeoEye throughout the experiment. The research was supported by the National Geospatial-Intelligence Agency and the National Science Foundation.

References

Aguilar, M.A., F.J. Aguilar, F. Agüera, and J.A. Sánchez, 2007. Geometric accuracy assessment of QuickBird Basic Imagery using different operational approaches, *Photogrammetric Engineering & Remote Sensing*, 73(12):1321–1332.

Di, K., R. Ma, and R. Li, 2003a. Rational functions and potential for rigorous sensor model recovery, *Photogrammetric Engineering & Remote Sensing*, 69(1):33–41.

Di, K., R. Ma, and R. Li, 2003b. Geometric processing of Ikonos stereo imagery for coastal mapping applications, *Photogrammetric Engineering & Remote Sensing*, 69(8):873–879.

Dial, G., 2000. Ikonos satellite mapping accuracy, *Proceedings of the 2000 Annual ASPRS Convention*, 22–26 May, Washington, D.C., unpaginated CD-ROM.

Fraser, C., 1999. Status of high resolution satellite imaging, *Proceedings of Photogrammetric Week '99* (D. Fritsch and D. Hobbie, editors), Wichmann Verlag, Heidelberg, pp. 117–123.

Fraser, C., and H. Hanley, 2003. Bias compensation in rational functions for Ikonos satellite imagery, *Photogrammetric Engineering & Remote Sensing*, 69(1):53–57.

Habib, A., S. Shin, K. Kim, C. Kim, K. Bang, E. Kime, and D. Lee, 2007. Comprehensive analysis of sensor modeling alternatives for high-resolution imaging satellites, *Photogrammetric Engineering & Remote Sensing*, 73(11):1241–1251.

Li, R., 1998. Potential of high resolution satellite imagery for national mapping products, *Photogrammetric Engineering & Remote Sensing*, 64(2):1165–1169.

Li, R., K. Di, and R. Ma, 2003. 3D shoreline extraction from Ikonos satellite imagery, *The 4th Special Issue on Marine & Coastal GIS - Journal of Marine Geodesy*, 26(1/2):107–115.

Li, R., F. Zhou, X. Niu, and K. Di, 2007. Integration of Ikonos and QuickBird Imagery for geopositioning accuracy analysis, *Photogrammetric Engineering & Remote Sensing*, 73(9):1067–1074.

Lutes, J., and J. Grodecki, 2004. Error propagation in Ikonos mapping blocks, *Photogrammetric Engineering & Remote Sensing*, 70(8):947–955.

Monteiro, L.S., T. Moore, and C. Hill, 2005. What is the accuracy of DGPS?, *The Journal of Navigation*, 58:207–225.

Niu, X., K. Di, J. Wang, J. Lee, and R. Li, 2004. Geometric modelling and photogrammetric processing of high-resolution satellite imagery, *Proceedings of the XXth Congress of International Society for Photogrammetry and Remote Sensing (ISPRS 2004)*, 12–23 July, Istanbul, Turkey.

Noguchi, M., C.S. Fraser, T. Nakamura, T. Shimono, and S. Oki, 2004. Accuracy assessment of QuickBird stereo imagery, *The Photogrammetric Record*, 19(106):128–137.

Tao, C.V., and Y. Hu, 2001. A comprehensive study of the rational function model for photogrammetric processing, *Photogrammetric Engineering & Remote Sensing*, 67(12):1347–1357.

Tao, C.V., Y. Hu, and W. Jiang, 2004. Photogrammetric exploitation of Ikonos imagery for mapping applications, *International Journal of Remote Sensing*, 25(14):2833–2853.

Wang, J., K. Di, and R. Li, 2005. Evaluation and improvement of geopositioning accuracy of IKONOS stereo imagery, *ASCE Journal of Surveying Engineering*, 13(2):35–42.

Zhou, G., and R. Li, 2000. Accuracy evaluation of ground points from Ikonos high-resolution satellite imagery, *Photogrammetric Engineering & Remote Sensing*, 66(9):1103–1112.

(Received 01 May 2008; accepted 01 August 2008; revised 05 November 2008)